Influence of secondary phases on ferroelectric properties of $Bi_{0.5}Na_{0.5}TiO_3$ ceramics

CrossMark

Andrea Prado-Espinosa[1], Miriam Castro, Leandro Ramajo*,[1]

Institute of Research in Materials Science and Technology (INTEMA) (CONICET-Universidad Nacional de Mar del Plata), Juan B. Justo 4302 (B7608FDQ), Mar del Plata, Argentina

ARTICLE INFO

ABSTRACT

The effects of secondary phases on ferroelectric properties of $Bi_{0.5}Na_{0.5}TiO_3$ (BNT) have been studied. Ceramic powders were prepared by solid state reaction employing different sintering temperatures and characterized by X-ray diffraction (XRD), Scanning Electron Microscopy and impedance spectroscopy. The perovskite structure was detected by XRD; together with small peaks corresponding to a secondary phase assigned to the $Na_2Ti_6O_{13}$-based phase in calcined powders. In addition, morphology and the content of the secondary phase were modified by the sintering temperatures, affecting the ferroelectric properties, and ac and dc conductivities. We believe that our results can benefit not only the understanding of BNT ceramics, but also expand the range of applications.

1. Introduction

Lead toxicity has become a serious environmental and health issue that cannot be overlooked. Therefore, legal restrictions on the use of lead in electric and electronic devices stimulated increasing efforts for the development of lead-free alternatives to lead zirconate titanate (PZT)-based piezoelectric ceramics [1,2]. However, lead-free materials do not show properties comparable to PZT piezoceramics. Furthermore, key properties such as piezoelectric coefficient (d_{33}) and depolarization temperature (T_d) need to be improved for practical applications.

Bismuth based titanates, such as $Bi_{0.5}Na_{0.5}TiO_3$(BNT) have been known and studied for decades but have not been fully used yet [3,4] due to the excellent properties of PZT ceramics. Although solid solutions of BNT ceramics, such as BNT-$BaTiO_3$ (BNBT), BNT-$Bi_{0.5}K_{0.5}TiO_3$ (BNKT), etc., are known for the formation of a morphotropic phase boundary (MPB), piezoelectric coefficient (d_{33}) and depolarization temperature (T_d) are not good enough to replace PZT ceramics [5,6].

Kainz et al. studied the solid-state reaction of BNT-based ceramics [7] and found that the perovskite phase can be obtained by the reaction of the starting materials and the intermediate phases. Indeed, oxides and carbonates react under evaporation of carbon dioxide to produce the stoichiometric perovskite (1-x)BNT–xBKT. In addition, the intermediate phase of bismuth titanate ($Bi_2Ti_2O_7$) may also be obtained

from bismuth oxide and titania [7]. The polytitanate intermediate phase ($M_2Ti_6O_{13}$, M=Na/K)) can be produced by the reaction of alkali carbonate and titania together with the evaporation of carbon dioxide. The two intermediate phases interact leading to stoichiometric perovskite and titania which in turn reacts with bismuth oxide and sodium carbonate to form stoichiometric perovskite. Knowing that secondary phases can be formed during sintering process and taking into account their possible influence on BNT final properties, a thorough understanding of local compositional variations on structure, microstructure and dielectric properties is needed.

In this work, we present a simple method to prepare $Bi_{0.5}Na_{0.5}TiO_3$-based lead-free piezoelectric ceramics through the solid-state reaction route. It is important to mention that these ceramics were sintered at different temperatures. As a result of these experiments, two main achievements were obtained. Firstly, it was possible to shed light on the effect of the sintering temperature on the structure and microstructure. Secondly, the influence of the secondary phase on the electric and dielectric properties of BNT-based ceramics was established.

2. Experimental procedure

$Bi_{0.5}Na_{0.5}TiO_3$ was synthesized through solid state reaction, using Na_2CO_3 (Cicarelli 99.99%; Argentina), Bi_2O_3 (Aldrich 99.8%; USA) and TiO_2 (Aldrich 99.9%; USA). Powders were mixed and milled using zirconia balls in an alcoholic medium of a planetary mill for 6 h

---

(Fritsch, Pulverisette 7, 1450 rpm). Powders were dried and calcined at 750 °C for 2 h. The resulting powders were milled again, pressed into disks and sintered at 1125 and 1150 °C for 2 h.

Crystalline phases were characterized by X-ray diffraction (XRD) (Philips PW1830), using CuK$_\alpha$ radiation, whereas density values were determined by the Archimedes method. Microstructures were evaluated on polished and thermally etched samples by Scanning Electron Microscopy (SEM), using a JEOL JSM-6460LV microscope equipped with energy dispersive spectroscopy, EDS.

Previous to the electrical measurements, samples were painted using a fired silver paste for the electric contacts. Dielectric properties were determined at different frequencies using an impedance analyzer (LCR meter HP4284A) over a frequency range of 100 Hz–1 MHz and in the temperature range from 20 to 500 °C. For the measurement of the piezoelectric constant the samples were first polarized inside a silicone bath using 2.5 kV/mm at 150 °C for 30 min, and the piezoelectric coefficients d$_{33}$ were recorded using a quasi-static piezoelectric d$_{33}$ meter (YE2730 – Sinoceramics). The dc conductivity was determined using an impedance analyzer Hioki DSM-8104. From the imaginary permittivity values (ε") at different frequencies, the ac conductivity (σ$_{ac}$) data can be calculated according to the following equation:

$$\sigma_{ac} = \varepsilon".\varepsilon_0.\omega \qquad (1)$$

being ε$_0$ = 8.85×10^{-12} F/m and ω=2.π. frequency.

3. Results and discussion

As mentioned before ceramics were sintered at two different temperatures (1125 and 1150 °C) in order to assess the structure of the BNT system. The X-ray diffraction patterns of the calcined powder at 750 °C and sintered ceramics are shown in Fig. 1. All diffraction patterns correspond to a perovskite-phase. However, slight traces of a minor secondary-phase can be seen, which are assigned to Na$_2$Ti$_6$O$_{13}$(NTO) (JCPDS nos. 14-0277) with monoclinic structure (hereafter, denoted as **NTO**), in the calcined powder. Although this secondary phase was also reported by Kainz et., the formation of the intermediate phase of bismuth titanate was not detected in sintered samples [7]. For these samples, the diffraction patterns correspond to a perovskite-phase with rhombohedral structure and lattice parameters a, b and c 5.476, 5.476, 6.778 (Å), respectively (JCPDS nos. 36-340). After analyzing the peaks of sintered samples located between 40° < 2θ < 42° and 46° < 2θ < 48° corresponding to the (003 and 021) and (202) planes (Fig. 1), the existence of a pure rhombohedral structure in all
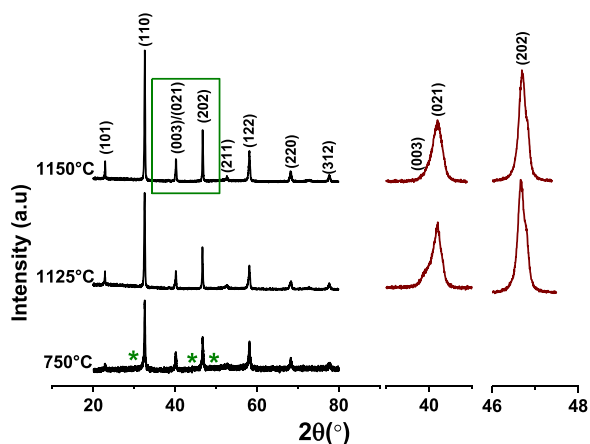

Fig. 1. XRD patterns of calcined powder at 750 °C for 2 h and ceramics sintered at 1125 and 1150 °C for 2 h. In the calcined powder, different peaks that are associated with the occurrence of the secondary phase appear and are signaled with (*) symbol. The insets of each figure show a detail of the XRD diffraction pattern in the 2θ range 40–42° and 46–48° of the BNT ceramics.

cases was established.

The SEM images, Fig. 2(**a-d**), illustrates the microstructure of the BNT ceramics, which were sintered at 1125 and 1150 °C for 2 h, respectively. From Fig. 2, it can be observed that the ceramics have dense microstructure, as shown in Table 1, in which pores are located mainly at grain boundaries and triple points. Triple points close to 120° indicate the sintering final stage where pores are removed by diffusion processes. The figure shows the typical BNT morphology consisting of big and uniform grains with small traces of secondary phases. Moreover, a rod-like secondary phase morphology homogenously distributed around the BNT surface on samples sintered at 1125 °C can be observed. When samples were sintered at 1150 °C, amorphous agglomerations of secondary phase of about 10 μm for BNT ceramics were detected.

Grain size distributions, **GSD**, of the ceramic samples are shown in the insets of Fig. 2(c-d). In the GSDs, it can be observed that grain size increases with the sintering temperature. The average grain size (**AGS**) increases from ~4.7 ± 2.8 μm in the ceramic at the lowest sintering temperature (1125 °C), to ~5.5 ± 4.0 μm for the ceramic sintered at 1150 °C. As the AGS evolves, the secondary phase morphology changes with thermal treatment.

EDS analyses were carried out on all the specimens in order to identify the composition of the BNT and **NTO** phase. Fig. 2(**a** and **b**) and Table 1 show the analysis of selected points for BNT ceramics sintered at 1125 and 1150 °C. Na, Bi, O and Ti ions were found in the matrix and their composition was confirmed to be very close to BNT (see composition table from EDS spectra). In the Na$_2$Ti$_6$O$_{13}$ phase, however, a low Bi amount has been expected (see composition table). Through the EDS analysis, the composition of the secondary phase is close to the Na$_2$Ti$_6$O$_{13}$-based phase with monoclinic structure.

The presence of voids, secondary phases and differences in the grain size could modify the dielectric performance of these samples. Specifically, interfacial polarization depends on the grain size and the possible formation of secondary phases. Table 1 shows density (ρ), piezoelectric coefficient (d$_{33}$), real permittivity (ε´) and dielectric loss (ε″) values of these samples. From dielectric properties and piezoelectric measurements, samples sintered at 1150 °C present the maximum values, due to their higher density and grain size. On the other hand, the d$_{33}$ value registered in samples sintered at 1150 °C is close to the value obtained in BNT [8], suggesting that, at this sintering temperature, density and polarization conditions were enough to obtain the best properties.

In order to observe the temperature and frequency dependence, Fig. 3 shows the relative permittivity and the dielectric loss as a function of temperature at various frequencies of samples sintered at 1125 and 1150 °C. The shift in the maximum temperature depending on frequency and the depolarization temperature, as well as the broadening of real permittivity peak around the dielectric maximum temperature due to compositional fluctuations occurring at A- and B-sites of the perovskite unit cell for all samples, suggests the relaxor-like behavior of these ceramics.

In addition, Fig. 3 shows, at low frequency (< 100 Hz), a broadening in real permittivity and a sharp increase in the dielectric loss with temperature. This behavior is more pronounced on ε´ curves in samples sintered at the highest temperature (1150 °C) and on ε″ curves in samples sintered at the lowest temperature (1125 °C), due to the conductivity effect and the secondary phase distribution on each sample. It is known that **NTO** structure presents TiO$_6$ octahedrons interconnected with each other by edges or corners forming both layer- and tunnel-structured sodium titanates (**NTO**), which facilitates Na-ion conductivity, and it is strongly influenced by temperature [9,10]. The apparition of this secondary phase could be related to the mechanochemical activation of powders in the solid-state reaction method [11]. As the secondary phase amount increases, conductivity and dielectric loss values at high temperature rise too. Moreover internal barrier layers could be formed when the grain size growths.
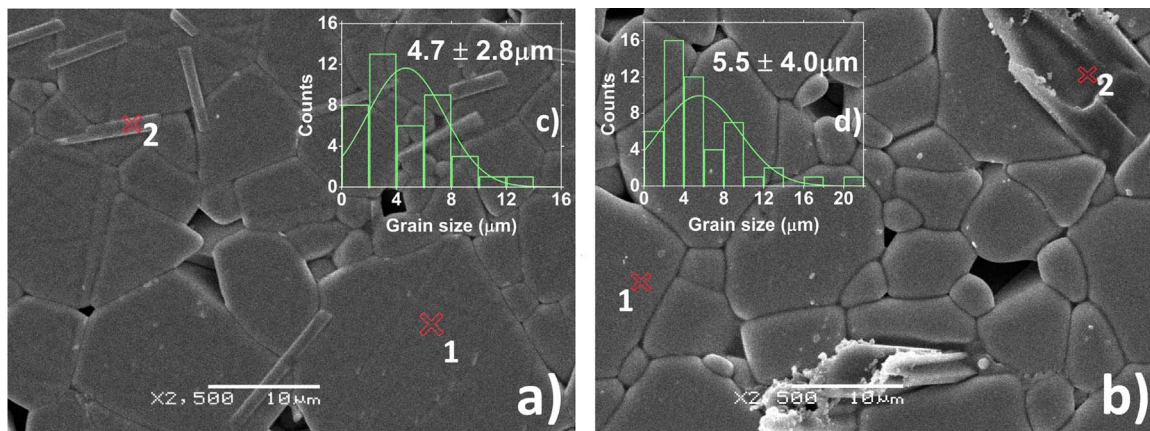
Fig. 2. SEM images of BNT ceramics sintered at 1125 °C (a) and 1150 °C (b) for 2 h. The inserts of Fig. (c and d) show the grain-size distributions of BNT ceramics.

Table 1
The table shows the composition on the regions illustrated in Fig. 2 derived from EDS spectra, which represent the atomic percentages of elements. Moreover, the table presents the relative density (ρ), piezoelectric coefficient (d_{33}), dielectric constant (ε') and dielectric loss (ε'') of the BNT ceramic samples measured at 30 °C and 10 kHz.

Sample		O	Na	Bi	Ti	ρ (g/cm^3)	d_{33} (pC/N)	ε'	ε''
BNT−1125	1	2.91	0.64	0.42	1.03	5.63 ± 0.10	57	566	0,0741
	2	13.42	2.33	0.25	4.72				
BNT−1150	1	2.57	0.67	0.64	1.16	5.76 ± 0.05	80	690	0,0518
	2	11.81	2.32	0.00	7.09				
BNT stoichiometric composition [9]		3	0.5	0.5	1	5.99	67 ± 10	423	0.0500
NTO Na$_2$Ti$_6$O$_{13}$		13	2	0	6	3.51 (JCPDS Nos. 14–0277)	−	−	−
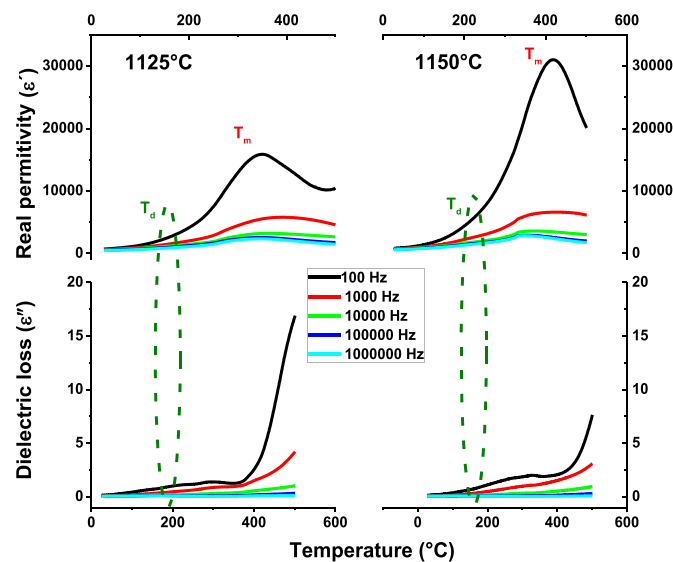
Fig. 3. Real permittivity (ε', top) and dielectric loss (ε'', bottom) vs. temperature curves of BNT-1125 °C and BNT-1150 °C samples obtained at different frequencies.

These layers contribute to the formation of internal barrier layer capacitors (IBLC) [12] improving the dielectric properties. Consequently, the better dispersion and alignment of NTC in BNT sintered at 1150 °C form more microcapacitors, increasing the dielectric constants.

Finally, Table 2 shows dc and ac conductivity (σ_{dc} and σ_{ac}) values of the sintered samples at different temperatures. A clear influence of temperature on ac and dc conductivity processes can be observed. Effectively, samples sintered at low temperature (1125 °C) show an important change in these processes. This behavior can be correlated with the significant dielectric loss increasing when temperature rises

Table 2
The table shows the dc and ac conductivities (σ_{dc} and σ_{ac}) of the BNT ceramic samples measured at different temperatures, 10 kHz and 250 V.

MUESTRA		$T_{30\,°C}$	$T_{110\,°C}$	$T_{150\,°C}$	$T_{210\,°C}$
BNT−1125 °C	σ_{dc} (10^{-9}S m^{-1})	5.57	49	202	3465
	σ_{ac} (10^{-9}S m^{-1})	2.33	4.08	9.13	16.9
BNT−1150 °C	σ_{dc} (10^{-9}S m^{-1})	17.0	20.0	40	148
	σ_{ac} (10^{-9}S m^{-1})	1.99	4.36	8.16	8.96

(see Fig. 3 for BNT-1125 °C).

Electrical modulus (Eq. (2)) is frequently used to understand relaxation processes which appear at low frequencies [13].

$$M^*(\omega) = \frac{1}{\varepsilon_r^*} = \frac{\varepsilon_r'}{\varepsilon_r'^2 + \varepsilon_r''^2} + \frac{i\varepsilon_r''}{\varepsilon_r'^2 + \varepsilon_r''^2} = M' + M'' \tag{2}$$

Fig. 4 shows the imaginary (M′′) part of electrical modulus for BNT samples sintered at 1125 and 1150 °C. Peaks in M′′ curves, which are not evident from loss tangent curves, indicate that a relaxation process can be observed. These peaks correspond to two relaxation processes and are displaced to higher frequencies when temperature increases. Relaxation peaks fall into the low frequency range (100 to10^5 Hz), and high frequency range (f10^5 Hz). These phenomena are associated with the contribution of the capacitance to structural or material characteristics (low frequency) and grain phase (high frequency) [14]. Moreover, the peak of the imaginary part of the electrical modulus, at low frequencies, is affected by changes in the stabilized structure. When temperature rises to the maximum temperature (T_m), a decrease in this value is observed. However, at
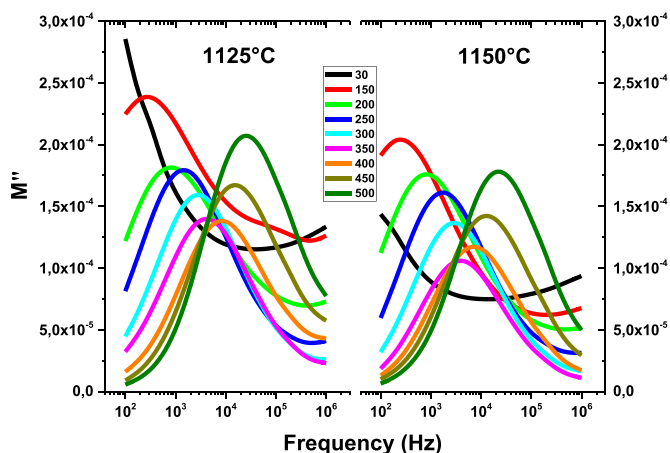
Fig. 4. Variation of M″ with frequency of BNT-1125 °C and BNT-1150 °C samples at different temperatures (30–500 °C).
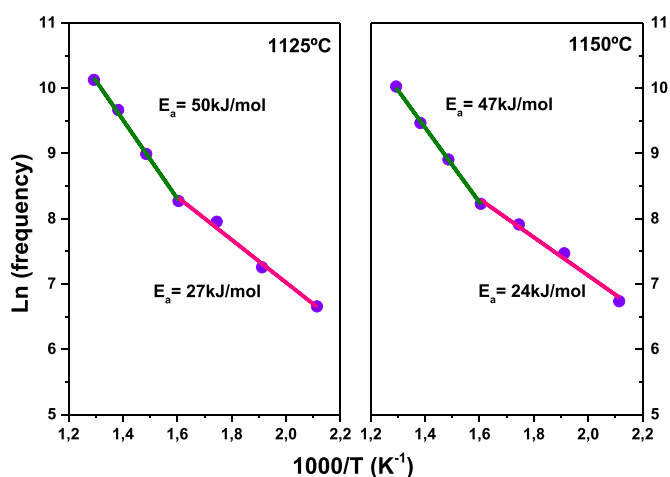

Fig. 5. Arrhenius plots of BNT-1125 °C and BNT-1150 °C samples.

temperatures higher than T_m, the maximum value increases. This peak indicates the transition of long range to short-range mobility with a raise in frequency [15].

From Fig. 4, frequencies corresponding to the maximum imaginary part of electrical modulus at the different temperatures can be extracted. Consequently, Arrhenius plots of frequency are displayed in Fig. 5, and activation energies of the relaxation processes in BNT-samples are obtained. Variations in the activation energy have been associated with the transition from the ferroelectric state to the so-called "anti-ferroelectric" where the depolarization temperature is registered. It is important to mention that, both sintered samples show similar activation energies indicating, that the same relaxation process proceeds.

4. Conclusions

The effect of secondary phases, in particular $Na_2Ti_6O_{13}$, on ferroelectric properties of $Bi_{0.5}Na_{0.5}TiO_3$ (BNT) ceramics, obtained by the conventional mixed oxide method, has been reported. Ceramic powders were prepared using different sintering temperatures in order to obtain a different content and morphology of the secondary phase. The structural and microstructural analyses show the formation of a main perovskite-type structure and a secondary phase with composition close to $Na_2Ti_6O_{13}$. Indeed, when the sintering temperature is raised, the secondary phase content increases and changes on its morphology are detected. Owing to the $Na_2Ti_6O_{13}$ structure, conductivity and dielectric properties at low frequency are increased. From conductivity measurements and SEM images, the effect of the NTO secondary phase on electric properties can be assigned. This secondary phase could not be detected through XRD patterns of sintered samples. As a result, we believe that knowledge of the characteristics secondary phases can be advantageous in the development of BNT based materials.

Competing financial interests

The authors declare no competing financial interests.

Acknowledgments

References

[1] J. Rödel, W. Jo, K.T.P. Seifert, E.-M. Anton, T. Granzow, D. Damjanovic, Perspective on the development of lead-free piezoceramics, J. Am. Ceram. Soc. 92 (2009) 1153–1177.

[2] X.P. Jiang, L.Z. Li, M. Zeng, H.L.W. Chan, Dielectric properties of Mn-doped $(Na_{0.8}K_{0.2})_{0.5}Bi_{0.5}TiO_3$ ceramics, Mater. Lett. 60 (2006) 1786–1790.

[3] V.A. Isupov, Ferroelectric $Na_{0.5}Bi_{0.5}TiO_3$ and $K_{0.5}Bi_{0.5}TiO_3$ Perovskites and Their Solid Solutions, Ferroelectrics 315 (2005) 123.

[4] Z.H. Zhou, J. Xue, W. Li, J. Wang, H. Zhu, J. Miao, Ferroelectric and electrical behavior of $(Na_{0.5}Bi_{0.5})TiO_3$ thin films, Appl. Phys. Lett. 85 (2004) 804.

[5] H. Yu, Z.G. Ye, Dielectric, ferroelectric, and piezoelectric properties of the lead-free $(1−x)(Na_{0.5}Bi_{0.5})TiO_3-xBiAlO_3$ solid solution, Appl. Phys. Lett. 93 (2008) 112902.

[6] D. Lin, D. Xiao, J. Zhu, P. Yu, Piezoelectric and ferroelectric properties of $[Bi_{0.5}(Na_{1−x−y}K_xLi_y)_{0.5}]TiO_3$ lead-free piezoelectric ceramics, Appl. Phys. Lett. 88 (2006) 062901.

[7] T. Kainz, M. Naderer, D. Schütz, O. Fruhwirth, F.A. Mautner, K. Reichmann, Solid state synthesis and sintering of solid solutions of BNT−xBKT, J. Eur. Ceram. Soc. 34 (2014) 3685–3697.

[8] J. Trelcat, C. Courtois, M. Rguiti, A. Leriche, P. Duvigneaud, T. Segato, Morphotropic phase boundary in the BNT−BT−BKT system, Ceram. Int. 38 (2012) 2823–2827.

[9] X. Wang, Y. Li, Y. Gao, Z. Wang, L. Chen, Additive-free sodium titanate nanotube array as advanced electrode for sodium ion batteries, Nano Energy 13 (2015) 687–692.

[10] L. Zhen, C.Y. Xu, W.S. Wang, C.S. Lao, Q. Kuang, Electrical and photocatalytic properties of $Na_2Ti_6O_{13}$ nanobelts prepared by molten salt synthesis, Appl. Surf. Sci. 255 (2009) 4149–4152.

[11] F. Rubio-Marcos, J.J. Romero, M.S. Martín-Gonzalez, J.F. Fernández, Effect of stoichiometry and milling processes in the synthesis and the piezoelectric properties of modified KNN nanoparticles by solid state reaction, J. Eur. Ceram. Soc. 30 (2010) 2763–2771.

[12] L. Ramajo, R. Parra, J.A. Varela, M.M. Reboredo, M.A. Ramírez, M.S. Castro, Influence of vanadium on electrical and microstructural properties of $CaCu_3Ti_4O_{12}/CaTiO_3$, J. Alloy. Compd. 497 (2010) 349–353.

[13] F. Tian, O. Ohki, Electric modulus powerful tool for analyzing dielectric behavior, IEEE Trans. Dielectr. Electr. Insul. 21 (2014) 929–931.

[14] L. Singh, W. Kim, B.C. Sin, A. Ullah, S.K. Woo, Y. Lee, Study of dielectric, AC-impedance, modulus properties of $0.5Bi0.5Na0.5TiO3·0.5CaCu3Ti4O12$ nano-composite synthesized by a modified solid state method, Mater. Sci. Semicond. Process 31 (2015) 386–396.

[15] B.K. Baricka, R.N.P. Choudhary, D.K. Pradhan, Dielectric and impedance spectroscopy of zirconium modified $(Na_{0.5}Bi_{0.5})TiO_3$ ceramics, Ceram. Int. 39 (2013) 5695–5704.